The formulation of quantum statistical mechanics based on the Feynman path centroid density. V. Quantum instantaneous normal mode theory of liquids

Jianshu Cao and Gregory A. Voth
Department of Chemistry, University of Pennsylvania, Philadelphia, Pennsylvania 19104-6323

(Received 25 April 1994; accepted 24 June 1994)

The concept of instantaneous normal modes in liquids is extended into the quantum regime using the Feynman path centroid perspective in quantum statistical mechanics. To accomplish this goal, the variational quadratic approximation for the effective centroid potential is recast in a general multidimensional phase space form. In the context of the effective quadratic approximation, the velocity autocorrelation functions of liquids can then be predicted based on a set of instantaneous *quantum* normal modes. Representative applications are presented for quantum Lennard-Jones liquids and a quantum particle solvated in a classical fluid. The quantum effective phonon spectrum leads to some revealing observations and interpretations for these systems.

I. INTRODUCTION

In the framework of condensed matter theory,[1,2] the concept of phonons, i.e., the small oscillations about a stable structure or the energy minimum, relates directly to many equilibrium properties and transport processes such as heat capacity, thermal conductivity, thermal expansion, light scattering, etc. Liquids, however, differ from solids because of their lack of static and stable structures. The fluidity of liquids thereby makes it formally improper to apply the well-developed theory of phonons. Yet, since the phonon spectrum in solids gives the eigenfrequencies of the phonons, one can speculate that the peaks in a liquid spectrum might offer some insight into the physical modes which characterize the liquid. Indeed, macroscopic measurements, such as the Fourier transformation of the velocity time correlation function, must contain information on the underlying dynamics of the liquid phase.[3] Because liquids exhibit diffusive properties, however, it remains a challenge to derive a set of modes which predict molecular motion in liquids from a microscopic point of view.[4] Nevertheless, liquids might behave similarly to solids for times smaller than some phenomenological relaxation time "τ". As a result, the concept of "instantaneous normal modes" (INM) remains useful during the lifetime of such solid-like behavior. Several authors have explored this intriguing picture of liquids.[5–11]

The INM approach suggests a liquid state analogy to the phonon spectrum in solids. However, rather than solving for the small oscillations at the global potential minimum, the liquid state potential is Taylor expanded at instantaneous configurations of liquids through quadratic order. A set of normal modes is then obtained by diagonalizing the force-constant matrix and the short-time dynamics resulting from that liquid configuration can be predicted. While the potential which determines the equilibrium structure of liquid is far from harmonic, the short-time motion of the molecules is nevertheless linear for a time interval shorter than the relaxation time τ. This effective harmonic motion is suggested to persist up to the characteristic relaxation time, at which point it is transformed into motion characteristic of another set of instantaneous normal modes. The overall short-time dynamics of the liquid is thereby determined by a superposition of the harmonic motions of all possible configurations. The liquid state "phonon spectrum" is thus taken to be the ensemble average of the instantaneous normal modes of the liquid configurations.

Though the short-time normal mode analysis is at best a qualitative model to study transport properties, it can successfully reveal some distinct features of liquids. Unlike solids, the liquid INM configuration is not at a local minimum, so the force will therefore not vanish. Moreover, the force constant matrix will have negative eigenvalues corresponding to unstable normal modes. It can be argued that the fraction of unstable modes is the manifestation of the fluidity of liquids and the peak position of those modes is related to the size of the self-diffusion constant.[6]

Instantaneous normal modes have also been used to study the short-time dynamics of coupled translational and rotational motions in molecular fluids.[8] The predictions of the short-time harmonic motion were compared with exact molecular dynamics (MD) simulation results and found to agree only for very short times. As a result of the anharmonicity in the liquid, the difficulty in describing such correlation functions with the INM theory arises due to the presence of the unstable modes which diverge exponentially with time. From this point of view, it is mainly the unstable modes which destroy the linear motion of liquid. Since the imaginary frequencies presumably become operational after the characteristic relaxation time, it is perhaps reasonable to remove the unstable modes from the INM correlation function. Reasonable agreement with the shorter time behavior of correlation functions was obtained when this method was implemented.[8]

 0021-9606/94/101(7)/6184/9/$6.00 © 1994 American Institute of Physics

Downloaded 27 Mar 2001 to 18.60.2.110. Redistribution subject to AIP copyright, see http://ojps.aip.org/jcpo/jcpcr.jsp

The present paper extends the instantaneous normal mode picture of liquids into the quantum regime. This extension is of particular interest because, as opposed to the classical case, the quantum *dynamics* of liquid state systems are extremely difficult to study by exact numerical methods. Therefore, the present work has both a formal and a practical bent to it. This paper is the fifth in a series[12–15] (hereafter referred to as Papers I–IV) which explores the static[12] and dynamical[13–15] properties of quantum equilibrium systems within the context of the path centroid variable[16–20] in Feynman path integration.[21–28] In addition to a number of other things, Papers I–IV contain the basic elements necessary to extend the instantaneous normal mode picture of liquids into the quantum regime. For example, Paper I develops the formally exact theory for the centroid density which goes beyond the well-known Feynman–Hibbs' quasiclassical theory[22] by employing a resummed and renormalized diagrammatic perturbation expansion. This analysis explores the diagrammatic representations of various approximation schemes, including the effective quadratic variational approximation[17–20] which forms the imaginary time basis for quantum instantaneous normal modes. The focus of Paper II is on the challenging task of calculating quantum dynamical time correlation functions. Consistent with the theme of Paper I, real time dynamical information is extracted in Paper II from the analytical continuation of centroid-constrained imaginary time correlation functions so that the time correlation functions are expressed as the centroid density-weighted superposition of locally optimized harmonic time correlation functions. In Paper III, the centroid picture was extended to phase space and formulated for many degrees of freedom using a compact vector–matrix notation. The latter formulation will be employed in the present paper.

The quantum instantaneous normal mode picture of the present work should not be confused with the particularly fruitful and intuitive outgrowth of the centroid analysis called *centroid molecular dynamics*.[13–15,29] In the latter method, the motion of the quantum centroid variable is governed by classical-like dynamics generated by the centroid force which is derived from the mean centroid potential (cf. the justification in Paper III). Centroid molecular dynamics is not the topic of this paper.

The following sections are organized as follows: In Sec. II, the effective harmonic theory for the phase space centroid density is presented for the one-dimensional case and then extended to many dimensions. In the context of the centroid theory, quantum velocity correlation functions and self-diffusion constants[3,30] are also discussed. The quantum instantaneous normal mode picture is next presented in Sec. III and applied in Sec. IV to two kinds of physical systems: nearly classical quantum Lennard-Jones fluids and quantum particles solvated in classical solvents. The quantum and classical phonon spectra are compared and discussed in each case. Concluding remarks are given in Sec. V.

I. EFFECTIVE HARMONIC THEORY

In Paper I, the imaginary time position correlation function was expressed in terms of the Feynman path centroid density in coordinate space and the centroid-constrained imaginary time position correlation function $C_c(\tau,q_c)$. The former quantity defines the statistical distribution in the theory, while the latter function defines, among other things, the effective quantum width of the classical-like centroid "particle." In Paper III, the one-dimensional formalism of Paper I was extended into phase space so that the momentum is treated as an independent dynamical variable. Before proceeding to the variational effective harmonic representation of these quantities, some notation and definitions will be reviewed.

For a physical system consisting of N particles (or molecular sites), there are N three-dimensional particle positions $(\vec{q}_1,\ldots,\vec{q}_N)$ and N three-dimensional particle momenta $(\vec{p}_1,\ldots,\vec{p}_N)$. These variables will be represented by a single vector $\vec{\zeta}$ which is defined as the collection of the $6N$ degrees of freedom in phase space, $\vec{\zeta}=(\vec{p}_1,\ldots,\vec{p}_N,\vec{q}_1,\ldots,\vec{q}_N)$. The phase space centroid density as defined in Paper III is given by

$$\rho_c(\vec{\zeta}_c)=\int\cdots\int \mathscr{D}\vec{\zeta}(\tau)\,\delta(\vec{\zeta}_c-\vec{\zeta}_0)\exp\{-S[\vec{\zeta}(\tau)]/\hbar\}, \tag{2.1}$$

where the phase space centroid vector is given by

$$\vec{\zeta}_0=\frac{1}{\hbar\beta}\int_0^{\hbar\beta} d\tau\,\vec{\zeta}(\tau). \tag{2.2}$$

The action functional for the imaginary time phase-space path integral is given by[24]

$$S[\vec{\zeta}(\tau)]=\int_0^{\hbar\beta} d\tau\left(\frac{1}{2}\,\vec{p}\cdot(\tau)\mathbf{m}^{-1}\cdot\vec{p}(\tau)-i\vec{p}(\tau)\cdot\dot{\vec{q}}(\tau)\right.$$
$$\left.+V[\vec{q}(\tau)]\right), \tag{2.3}$$

where $\dot{\vec{q}}(\tau)$ is the imaginary time velocity vector, $\mathbf{m}$ is the diagonal particle mass matrix, and it has been assumed that the potential is defined to be independent of the momentum. The quantum partition function Z is calculated from Eq. (2.1) by taking the classical-like centroid trace, i.e., $Z=\int d\vec{\zeta}_c\rho_c(\vec{\zeta}_c)$. The centroid-constrained correlation function matrix is defined by[14]

$$\mathbf{C}_c(\tau,\vec{q}_c)=\frac{\int\cdots\int\mathscr{D}\vec{\zeta}(\tau)\,\delta(\vec{\zeta}_c-\vec{\zeta}_0)[\vec{\zeta}(\tau)-\vec{\zeta}_0][\vec{\zeta}(0)-\vec{\zeta}_0]\exp\{-S[\vec{\zeta}(\tau)]/\hbar\}}{\int\cdots\int\mathscr{D}\vec{\zeta}(\tau)\,\delta(\vec{\zeta}_c-\vec{\zeta}_0)\exp\{-S[\vec{\zeta}(\tau)]/\hbar\}} \tag{2.4}$$

Downloaded 27 Mar 2001 to 18.60.2.110. Redistribution subject to AIP copyright, see http://ojps.aip.org/jcpo/jcpcr.jsp

with each element of this matrix having the indices "i,j" being given explicitly by the 2×2 block

$$[\mathbf{C}_c(\tau,\vec{q}_c)]_{ij}=\begin{pmatrix} C_c[\tilde{p}_i(\tau)\tilde{p}_j(0),\vec{q}_c] & C_c[\tilde{p}_i(\tau)\tilde{q}_j(0),\vec{q}_c] \\ C_c[\tilde{q}_i(\tau)\tilde{p}_j(0),\vec{q}_c] & C_c[\tilde{q}_i(\tau)\tilde{q}_j(0),\vec{q}_c] \end{pmatrix}, \tag{2.5}$$

where $\vec{\tilde{\zeta}}(\tau)$ is the quantum path fluctuation with respect to the centroid variable $\vec{\zeta}_c$, i.e., $\vec{\zeta}(\tau)=\vec{\zeta}_c+\vec{\tilde{\zeta}}(\tau)$. The elements of the centroid-constrained correlation function matrix in Eq. (2.5) can also be calculated by first incorporating the external field terms $-\vec{f}(\tau)\cdot\vec{\tilde{q}}(\tau)$ and $-\vec{g}(\tau)\cdot\vec{\tilde{p}}(\tau)$ into the action functional [Eq. (2.3)] and then functionally differentiating the functional with $\exp\{-\beta F_c[\vec{f}(\tau),\vec{g}(\tau)]$ two times with respect to the desired combination of $f(\tau)$ and $g(\tau)$ and multiply by $\hbar^2/\rho_c$ in the limit $\vec{f}(\tau)\to0$ and $\vec{g}(\tau)\to0$. Here, $F_c[\vec{f}(\tau),\vec{g}(\tau)]\equiv-k_BT\ln\{\rho_c[\vec{f}(\tau),\vec{g}(\tau)]\}$ is the quantum centroid free energy written as a functional of the two external fields.

A. One-dimensional systems

For simplicity, a one-dimensional system will be first considered in this subsection, in which case p and q are one-dimensional variables and $\vec{\zeta}$ is a two-dimensional vector. In the case of an effective harmonic reference potential,[12,17,18,20] both the centroid density and the 2×2 centroid-constrained correlation function matrix $C_c(\tau,q_c)$ can be evaluated analytically. To do this, a Fourier decomposition of the phase space path fluctuation vector $\vec{\tilde{\zeta}}=(p,q)$ is introduced such that

$$\vec{\tilde{\zeta}}(\tau)=\sum_{n\neq0}\vec{\tilde{\zeta}}_n e^{-i\Omega_n\tau}, \tag{2.6}$$

with Ω_n being the Matsubara frequency defined by $\Omega_n=2\pi n/\hbar\beta$. The phase space action in Eq. (2.3) can then be rewritten as

$$S[\zeta(\tau)]=S_0[\vec{\zeta}_c+\vec{\tilde{\zeta}}(\tau)]+\beta\hbar\sum_{n\neq0}\left(\frac{|\hat{p}_n|^2}{2m}+\Omega_n\hat{p}_n\hat{q}_n^*+\frac{1}{2}m\omega_c^2|\hat{q}_n|^2\right), \tag{2.7}$$

where ω_c is the centroid-dependent frequency of the effective harmonic oscillator, and S_0 contains the remaining terms in the action

$$S_0=\beta\hbar\left\{\frac{p_c^2}{2m}+V[q_c+\tilde{q}(\tau)]-\frac{1}{2}m\omega_c^2\tilde{q}(\tau)^2\right\}. \tag{2.8}$$

This expression shows that the centroid momentum p_c is decoupled from the position coordinates provided the potential is not momentum dependent.[13,14,29] To be consistent with the vector–matrix notation, a generalized Gaussian width matrix $\mathbf{\Lambda}$ can be introduced here, given by

$$\mathbf{\Lambda}_n^{-1}=\beta\begin{pmatrix} m^{-1} & \Omega_n \\ -\Omega_n & m\omega_c^2 \end{pmatrix} \tag{2.9}$$

so that the action in Eq. (2.7) takes on the compact form

$$S=S_0+\frac{\hbar}{2}\vec{\tilde{\zeta}}_n\cdot\mathbf{\Lambda}_n^{-1}\cdot\vec{\tilde{\zeta}}_n. \tag{2.10}$$

The effective harmonic potential approximation assumes that S_0 depends only on the centroid variables.[12,17,18,20] With the help of the Gibbs–Bogoliubov–Feynman variational principle[31] or a renormalization of the diagrammatic perturbation theory for the centroid density (see Paper I), it can be shown that the effective harmonic potential is determined by optimizing the frequency ω_c as a function of the centroid position. This optimized frequency is given from the solution to the transcendental equation[12,17,18,20]

$$m\omega_c^2=\langle V''(q_c+\tilde{q})\rangle_\alpha=\frac{1}{\sqrt{2\pi\alpha_c}}\int d\tilde{q}\ V''(q_c+\tilde{q})\times\exp(-\tilde{q}^2/2\alpha_c), \tag{2.11}$$

where the Gaussian width for a particular centroid position is

$$\alpha_c=\frac{1}{\beta m\omega_c^2}\left[\frac{\hbar\beta\omega_c/2}{\tanh(\hbar\beta\omega_c/2)}-1\right]. \tag{2.12}$$

At this level of approximation, the action $S_0(\zeta_c)$ becomes

$$S_0=\beta\hbar\left[\frac{p_c^2}{2m}+V_{\rm eff}(q_c)\right], \tag{2.13}$$

which is a function only of the two phase space centroid variables and therefore independent of the variables $\vec{\tilde{\zeta}}(\tau)$. As a result, the centroid-constrained propagator in Eq. (2.4) is solely determined by the matrix terms $\mathbf{\Lambda}_n$,

$$\mathbf{C}_c(\tau,\zeta_c)=\sum_{n\neq0}\mathbf{\Lambda}_n(q_c)e^{-i\Omega_n\tau}, \tag{2.14}$$

where $\mathbf{\Lambda}_n$ is the inverse of Eq. (2.9), i.e.,

$$\mathbf{\Lambda}_n=\frac{1}{\beta(\omega^2+\Omega_n^2)}\begin{pmatrix} m\omega_c^2 & -\Omega_n \\ \Omega_n & m^{-1} \end{pmatrix}. \tag{2.15}$$

The dependence here on the centroid q_c comes implicitly through the optimized frequency ω_c defined in Eq. (2.11).

By carrying out the summation in Eq. (2.14) to infinite order, one obtains the optimized harmonic approximation for the centroid-constrained correlation function matrix

$$\mathbf{C}_c(\tau,q_c)=\begin{pmatrix} (m\omega_c)^2\alpha_c(\tau) & -\frac{1}{2}i\hbar\gamma_c(\tau) \\ \frac{1}{2}i\hbar\gamma_c(\tau) & \alpha_c(\tau) \end{pmatrix}. \tag{2.16}$$

In this expression, the centroid-constrained imaginary time position correlation function is explicitly given by

$$[\mathbf{C}_c(\tau,q_c)]_{22}=\alpha_c(\tau)=\frac{1}{\beta m\omega_c^2}\left(\frac{b_c/2}{\sinh(b_c/2)}\times\cosh[b_c(1/2-u)]-1\right), \tag{2.17}$$

where $u=\tau/\hbar\beta$ and $b_c=\hbar\beta\omega_c$. At this level of approximation, the function $\gamma_c(\tau)$ in the off-diagonal terms of Eq. (2.16) reads

Downloaded 27 Mar 2001 to 18.60.2.110. Redistribution subject to AIP copyright, see http://ojps.aip.org/jcpo/jcpcr.jsp

$$\gamma_c(\tau)=\frac{\sinh[b_c(1/2-u)]}{\sinh(b_c/2)}. \tag{2.18}$$

By integrating the above expressions over the normalized phase space centroid density $\rho_c(\vec{\zeta}_c)/Z$, i.e.,

$$\langle\zeta_i(\tau)\zeta_j(0)\rangle=\langle[\mathbf{C}_c(\tau,q_c)]_{ij}+\zeta_{c,i}\zeta_{c,j}\rangle_{\rho_c}, \tag{2.19}$$

one can obtain the effective harmonic expressions for the different imaginary time phase space correlation functions from Eq. (2.16). In the above equation, $\zeta_{c,1}$ and $\zeta_{c,2}$ equal p_c and q_c respectively.

Some simple results immediately follow from Eq. (2.16) using the Gaussian representation of operators and imaginary time correlation functions developed in Papers II and III. For example, the adherence to the Uncertainty Principle in the effective harmonic theory can be demonstrated by evaluating the Heisenberg commutator

$$\langle[q,p]\rangle=\lim_{\tau\to 0}\langle C_c[\tilde{q}(\tau)\tilde{p}(0)]-C_c[\tilde{p}(\tau)\tilde{q}(0)]\rangle_{\rho_c}=i\hbar. \tag{2.20}$$

In addition, the average kinetic energy is found to be given by

$$\left\langle\frac{p^2}{2m}\right\rangle=\frac{1}{2m}\langle(p_c+\tilde{p})^2\rangle=\frac{1}{2\beta}\left\langle\frac{b_c/2}{\tanh(b_c/2)}\right\rangle_{\rho_c} \tag{2.21}$$

which is the same expression as a virial estimator for the kinetic energy derived previously.[20]

B. Multidimensional systems

The analysis in the preceding subsection can be generalized to treat a system consisting of N particles in three-dimensional space (see also the Appendix of Paper I and Sec. III of Paper IV). A $3N\times 3N$ force constant matrix is first defined as

$$[\mathbf{K}(\vec{q})]_{ij}=\frac{\partial^2 V(\vec{q})}{\partial q_i\partial q_j} \tag{2.22}$$

along with the Gaussian width matrix

$$[\mathbf{C}_c(0,\vec{q}_c)]_{ij}=C_c[\tilde{q}_i(0)\tilde{q}_j(0),\vec{q}_c] \tag{2.23}$$

which is simply a submatrix of $\mathbf{C}_c(\tau,\vec{q}_c)$ in Eq. (2.4) evaluated at $\tau=0$. Following the notation used in the previous papers,[12–15] the effective harmonic centroid force constant matrix is given by

$$\mathbf{K}_c(\vec{q}_c)=\langle\mathbf{K}(\vec{q}_c+\vec{\tilde{q}})\rangle_c=\frac{1}{\sqrt{\det[2\pi\mathbf{C}_c(\vec{q}_c)]}}\int d\vec{\tilde{q}}\times\mathbf{K}(\vec{q}_c+\vec{\tilde{q}})\exp[-\vec{\tilde{q}}\cdot\mathbf{C}_c^{-1}(\vec{q}_c)\cdot\vec{\tilde{q}}/2]. \tag{2.24}$$

From the above equation, it is clear that the Gaussian width matrix $\mathbf{C}_c(\vec{q}_c)$ is the multidimensional generalization to the centroid-constrained thermal width α_c in Eq. (2.12). At the level of the effective quadratic approximation, the Gaussian width matrix is given by

$$\mathbf{C}_c(0,\vec{q}_c)=\sum_{n\neq 0}[\beta\mathbf{m}\Omega_n^2+\beta\mathbf{K}_c(\vec{q}_c)]^{-1}, \tag{2.25}$$

where $\mathbf{m}$ is the $3N$-dimensional particle mass matrix.

A centroid-dependent unitary matrix $\mathbf{U}(\vec{q}_c)$ can be found which diagonalizes the mass-scaled centroid force constant matrix $\bar{\mathbf{K}}_c(\vec{q}_c)$, giving the eigenfrequencies

$$\mathbf{U}^\dagger(\vec{q}_c)\bar{\mathbf{K}}_c(\vec{q}_c)\mathbf{U}(\vec{q}_c)=\mathbf{I}\cdot\vec{\omega}_c^2, \tag{2.26}$$

where $\vec{\omega}_c^2$ is the column vector consisting of the centroid-dependent eigenvalues $\omega_{c,l}^2$ and $\mathbf{I}$ is the $3N$-dimensional identity matrix. The Gaussian width factor matrix in Eq. (2.23) is obtained from the relation

$$\mathbf{C}_c(\vec{q}_c)=\bar{\mathbf{U}}(\vec{q}_c)(\mathbf{I}\cdot\vec{\bar{\alpha}}_c)\bar{\mathbf{U}}^\dagger(\vec{q}_c), \tag{2.27}$$

where the elements of the centroid-dependent normal mode thermal width factor vector $\vec{\bar{\alpha}}_c$ are given by

$$\bar{\alpha}_{c,l}=\frac{1}{\beta\omega_{c,l}^2}\left(\frac{(\hbar\beta\omega_{c,l}/2)}{\tanh(\hbar\beta\omega_{c,l}/2)}-1\right) \tag{2.28}$$

and the mass-scaled, centroid-dependent matrix $\bar{\mathbf{U}}(\vec{q}_c)$ is given by

$$\bar{\mathbf{U}}(\vec{q}_c)=\mathbf{m}^{-1/2}\mathbf{U}(\vec{q}_c). \tag{2.29}$$

The set of optimized frequencies $\{\omega_{c,l}\}$ are obtained from the self-consistent solution to the transcendental matrix equations in Eqs. (2.24)–(2.29) at each centroid position.

Obviously, the multidimensional generalization of Eq. (2.9) is

$$\mathbf{\Lambda}_n^{-1}(\vec{q}_c)=\beta\begin{pmatrix}\mathbf{m}^{-1} & \Omega_n\mathbf{I}\\ -\Omega_n\mathbf{I} & \mathbf{K}_c(\vec{q}_c)\end{pmatrix}. \tag{2.30}$$

With the eigensolutions $\{\omega_{c,l}\}$ from Eq. (2.26) in hand, Eq. (2.30) can be rewritten in terms of a mass-scaled unitary matrix $\mathbf{S}(\vec{q}_c)$ as

$$\mathbf{\Lambda}_n^{-1}=\beta\mathbf{S}(\vec{q}_c)\begin{pmatrix}\mathbf{I} & \Omega_n\mathbf{I}\\ -\Omega_n\mathbf{I} & \mathbf{I}\cdot\vec{\omega}_c^2\end{pmatrix}\mathbf{S}^\dagger(\vec{q}_c), \tag{2.31}$$

where

$$\mathbf{S}(\vec{q}_c)=\begin{pmatrix}\mathbf{m}^{-1/2}\mathbf{U}(\vec{q}_c) & 0\\ 0 & \mathbf{m}^{1/2}\mathbf{U}(\vec{q}_c)\end{pmatrix}. \tag{2.32}$$

The substitution of Eq. (2.31) into Eq. (2.14) then leads to the expression for the $6N$-dimensional centroid-constrained phase space correlation function matrix $\mathbf{C}_c(\tau,\zeta_c)$ [Eq. (2.5)], i.e.,

$$\mathbf{C}_c(\tau,\vec{q}_c)=\mathbf{S}(\vec{q}_c)\times\begin{pmatrix}\mathbf{I}\cdot\vec{\omega}_c^2\cdot\vec{\bar{\alpha}}_c(\tau) & -\frac{1}{2}i\hbar\mathbf{I}\cdot\vec{\gamma}_c(\tau)\\ \frac{1}{2}i\hbar\mathbf{I}\cdot\vec{\gamma}_c(\tau) & \mathbf{I}\cdot\vec{\bar{\alpha}}_c(\tau)\end{pmatrix}\mathbf{S}^\dagger(\vec{q}_c), \tag{2.33}$$

where $\vec{\gamma}_c(\tau)$ and $\vec{\bar{\alpha}}_c(\tau)$ are the multidimensional vector generalizations of Eqs. (2.17) and (2.18), respectively. The individual elements of these vectors are given by

$$\bar{\alpha}_{c,l}(\tau)=\frac{\hbar^2\beta}{b_{c,l}^2}\left(\frac{b_{c,l}/2}{\sinh(b_{c,l}/2)}\cosh[b_{c,l}(1/2-u)]-1\right) \tag{2.34}$$

Downloaded 27 Mar 2001 to 18.60.2.110. Redistribution subject to AIP copyright, see http://ojps.aip.org/jcpo/jcpcr.jsp

and

$$\gamma_{c,l}(\tau)=\frac{\sinh[b_{c,l}(1/2-u)]}{\sinh(b_{c,l}/2)} \tag{2.35}$$

with $u=\tau/(\hbar\beta)$ and $b_l=\hbar\beta\omega_{c,l}$. Once the complete centroid constrained correlation function matrix in Eq. (2.33) is obtained, the appropriate average over the phase space centroid density allows one to obtain the imaginary time phase space correlation functions [cf. Eq. (2.19)].

C. Velocity correlation functions and diffusion constants

In Paper II, it was argued that the time integral of the centroid velocity time correlation function gives an approximation to the quantum self-diffusion constant D. The argument is partly based on the relation

$$\langle\vec{v}_{c,i}(t)\cdot\vec{v}_{c,i}(0)\rangle_{\rho_c}=-\frac{\partial^2}{\partial t^2}\langle\vec{q}_{c,i}(t)\cdot\vec{q}_{c,i}(0)\rangle_{\rho_c}, \tag{2.36}$$

where $\vec{v}_{c,i}(t)$ and $\vec{q}_{c,i}(t)$ are the three-dimensional centroid velocity and position vectors for a "tagged" particle i, and these vectors obey the classical-like equations of motion of centroid molecular dynamics.[13,14,29] This expression arises from the approximate Fourier relationship between centroid time correlation functions and the real part of quantum correlation functions for the general case, i.e.,[13,14]

$$\tilde{\bar{C}}_{AB}(\omega)=f(\omega)\tilde{C}^*_{AB}(\omega), \tag{2.37}$$

where A and B are arbitrary quantum operators and the factor $f(\omega)$ is given by

$$f(\omega)=\frac{\hbar\omega\beta/2}{\tanh(\hbar\omega\beta/2)}. \tag{2.38}$$

In Eq. (2.37), $\tilde{C}^*_{AB}(\omega)$ and $\tilde{\bar{C}}(\omega)$ are the Fourier transformations of the centroid time correlation function and the real part of the quantum correlation function, respectively. Since the diffusion constant is the zero frequency component of the Fourier transform of the velocity correlation functions,[3] the choice A, $B=\vec{v}_i$ in Eq. (2.37) immediately gives

$$D=\frac{1}{3}\int_0^\infty dt\langle\vec{v}_{c,i}(t)\cdot\vec{v}_{c,i}(0)\rangle_{\rho_c} \tag{2.39}$$

where the bracket denotes an average over the equilibrium normalized phase space centroid density for all degrees of freedom. The above expression is the Green–Kubo-like expression for the quantum self-diffusion constant in centroid dynamics. In Papers II and IV, the above formula was used within the context of the centroid molecular dynamics method. In Sec. III below, Eq. (2.39) will instead be employed within the context of the effective harmonic theory [Eqs. (2.21)–(2.29b)] to develop a quantum INM perspective for self-diffusion.

Before proceeding to the next section, another centroid dynamical point of view on the self-diffusion constant will be outlined. This perspective arises directly from the definition of the self-diffusion constant, i.e.,

$$\lim_{t\to\infty}\langle|\vec{q}_i(t)-\vec{q}_i(0)|^2\rangle=6Dt. \tag{2.40}$$

This expression, of course, indicates that the mean-squared displacement of the tagged particle is not bound as a function of time unless its diffusion constant vanishes. The above argument holds exactly for the quadratic reference potential approximation. Making use of Eq. (2.16) gives the relation between the Fourier transform of the centroid-constrained correlation functions

$$\tilde{C}_c(\vec{v}_{c,i}\cdot\vec{v}_{c,i},\omega)=\omega^2\tilde{C}_c(\vec{q}_{c,i}\cdot\vec{q}_{c,i},\omega). \tag{2.41}$$

which verifies Eq. (2.36) in the context of the centroid path integration. Then, combining Eqs. (2.40) and (2.41), one can write

$$D=\tfrac{1}{3}\lim_{\omega\to0}\tilde{C}(\vec{v}_i\cdot\vec{v}_i,\omega)=\tfrac{1}{3}\lim_{\omega\to0}\omega^2\tilde{C}(\vec{q}_i\cdot\vec{q}_i,\omega) \tag{2.42}$$

which implies $\lim_{\omega\to\infty}\tilde{C}(\vec{q}_i\cdot\vec{q}_i,\omega)\propto\omega^{-2}$, thus indicating diffusive behavior. Equations (2.39) and (2.40) are two alternatives for obtaining the diffusion constant D and will serve as the basis for the definition of quantum instantaneous normal modes in the next section.

III. INSTANTANEOUS NORMAL MODE ANALYSIS

A. Classical theory

In this subsection, the classical INM perspective[6–8] will be reviewed. Intrinsically, a liquid state potential is highly anharmonic, so there is no stable configuration around which to perform a Taylor series expansion. It is only in the short-time limit, typically in the picosecond range, that the behavior of liquid molecules mimics linear harmonic equations of motion. One can picture a liquid during such short time intervals as being globally "frozen" so that only small displacements are observed without any major changes in the gross overall structure. Thereby, the liquid during a short time can be described by a set of collective linear harmonic oscillators.[6]

If one considers a liquid configuration $\vec{q}_0$ at the instant $t=0$, one can expand the potential surface about this instantaneous configuration as[6,7]

$$V(\vec{q})=V(\vec{q}_0)+\vec{F}(\vec{q}_0)\cdot(\vec{q}-\vec{q}_0)+\tfrac{1}{2}(\vec{q}-\vec{q}_0)\cdot\mathbf{K}(\vec{q}_0)\cdot(\vec{q}-\vec{q}_0), \tag{3.1}$$

where the linear force vector $\vec{F}(\vec{q}_0)$ and the force constant matrix $\mathbf{K}(\vec{q}_0)$ are the first and second derivatives of the potential with respect to $\vec{q}_0$, respectively, that is,

$$F_i(\vec{q}_0)=\frac{\partial V(\vec{q}_0)}{\partial q_i} \tag{3.2}$$

and

$$K_{ij}(\vec{q}_0)=\frac{\partial^2 V(\vec{q}_0)}{\partial q_i\partial q_j}, \tag{3.3}$$

in which the index denotes the degree of freedom, and runs from 1 to $3N$. The rest of the linear algebra is now straightforward. The mass-scaled force constant matrix $\tilde{\mathbf{K}}(\vec{q}_0)$ can be diagonalized by a configuration-dependent unitary transformation, i.e.,

$$\mathbf{I}\cdot\vec{\omega}^2(\vec{q}_0)=\mathbf{U}^\dagger(\vec{q}_0)\tilde{\mathbf{K}}(\vec{q}_0)\mathbf{U}(\vec{q}_0), \tag{3.4}$$

Downloaded 27 Mar 2001 to 18.60.2.110. Redistribution subject to AIP copyright, see http://ojps.aip.org/jcpo/jcpcr.jsp

where $\{\omega_i\}$ are the set of configuration-dependent eigenfrequencies. From this expression and the INM approximation, the classical velocity correlation function for a tagged particle is given by

$$C_{\rm cl}(t)=\frac{1}{m\beta}\frac{1}{3N}\sum_{i=1}^{3N}\langle\cos[\omega_i(\vec{q}_0)t]\rangle, \tag{3.5}$$

where the average is taken over all liquid configurations and a homogeneous atomic fluid has been assumed here for simplicity.

From the above expression, one can define the density of states for the instantaneous normal modes, namely, the instantaneous phonon spectrum

$$D_{\rm cl}(\omega)=\frac{1}{3N}\sum_{i=1}^{3N}\langle\delta[\omega-\omega_i(\vec{q}_0)]\rangle. \tag{3.6}$$

Then, the INM velocity time correlation function in Eq. (3.5) is expressed as

$$C_{\rm cl}(t)=\frac{1}{m\beta}\int d\omega\, D_{\rm cl}(\omega)\cos(\omega t) \tag{3.7}$$

in which the integration is understood to also cover the imaginary frequency region. The INM spectrum can also be identified as the Fourier transformation of the INM velocity time correlation function.[6,7]

B. Quantum generalization

The centroid-based effective harmonic theory in Sec. II readily allows quantum mechanics to be incorporated into the INM perspective. To begin, the centroid-constrained normal mode correlation function in Eq. (2.34) can be analytically continued to real time ($\tau\rightarrow it$) for each centroid position. Then, Eq. (2.41) can be used to obtain the centroid-constrained effective harmonic velocity correlation function in real time, and this correlation function can, in turn, be used to approximate the real part of the velocity time correlation function via Eqs. (2.19) and (2.37). After this mathematical procedure, one obtains

$$C_{\rm qm}(t)=\frac{1}{m\beta}\frac{1}{3N}\sum_{l=1}^{3N}\langle f(\omega_{c,l})\cos[\omega_{c,l}(\vec{q}_c)t]\rangle_{\rho_c}, \tag{3.8}$$

where factor f is given by Eq. (2.38) and the centroid-dependent optimized frequencies $\omega_{c,l}$ are given from the self-consistent solution to Eqs. (2.24)–(2.29). A homogeneous atomic fluid has again been assumed.

The interpretation of the above equation is clear: the short-time quantum velocity time correlations are given by the centroid density-weighted superposition of quantum harmonic motions having frequencies optimized for each instantaneous centroid configuration. The centroid dependence of the frequencies is shown here explicitly. By analogy with the classical INM picture, the quantum normal mode spectrum $D_{\rm qm}(\omega)$ is defined in terms of centroid frequencies as

$$D_{\rm qm}(\omega)=\frac{1}{3N}\sum_{l=1}^{3N}\langle\delta[\omega-\omega_{c,l}(\vec{q}_c)]\rangle_{\rho_c}. \tag{3.9}$$

This result leads us to rewrite the quantum velocity correlation function as

$$C_{\rm qm}(t)=\frac{1}{m\beta}\int d\omega\, f(\omega)D_{\rm qm}(\omega)\cos(\omega t). \tag{3.10}$$

Hence, the centroid normal mode spectrum and the Fourier transformation of the quantum velocity time correlation are not the same but are related to each other via $f(\omega)$. Within the context of the optimized harmonic centroid potential, it is straightforward to identify the set of optimized frequencies for a given centroid position as being the quantum INM frequencies for that configuration. The average of those optimized frequencies over the centroid density yields the liquid state quantum phonon spectrum.

IV. APPLICATIONS

A. Quantum Lennard-Jones fluids

In Paper II, the diffusion process in quantum Lennard-Jones (LJ) fluids was studied using centroid molecular dynamics[13–15,29] and the classical and quantum diffusion constants were compared. As neon or argon are nearly classical fluids, the effective potential surface was taken to be the classical one with small centroid quantum corrections [see Eq. (4.5) of Paper II]. It was found that when the quantum mechanical nature of the LJ fluid is taken into account the diffusion constant is reduced by a small faction and the decrease in diffusion constant is inversely proportional to its mass. Needless to say, the leading quantum correction employed in the simulation of quantum LJ fluids can be a crude estimation of the true centroid potential. The locally optimized harmonic approximation in Eqs. (2.24)–(2.27) will give a more accurate representation of the centroid potential. It is precisely these equations which also yield the qualitative information provided by the quantum INM analysis outlined in the previous section.

In practice, the calculation of the multidimensional Gaussian average in the transcendental matrix equation Eq. (2.24) can be a difficult task unless it can be evaluated as a analytical function. Fortunately, $\mathbf{C}_c$, representing the quantum thermal fluctuations about the centroid variables, is a relatively small quantity except at extremely low temperatures (an electron being the exception, of course). Such "narrow" Gaussian widths allow one to Taylor expand the centroid force constant matrix with some confidence, giving

$$\mathbf{K}_c(\vec{q}_c)=\mathbf{K}(\vec{q}_c)+\tfrac{1}{2}\partial_i\cdot\partial_j\mathbf{K}(\vec{q}_c):\mathbf{C}_c(\vec{q}_c), \tag{4.1}$$

where ∂_i is the partial derivative with respect to the ith degree of freedom. The force constant matrix $K(\vec{q}_c)$ is a $3N\times 3N$ matrix, the next term is a contraction of a fourth-order tensor and a matrix, and so on. Consequently, the computational effort in obtaining the optimized solution to Eqs. (2.24)–(2.27) scales as $(3N)^{2l}$, l being the order of Taylor expansion. In order to maintain computational efficiency while maintaining reasonable accuracy, a second-order Taylor expansion has been used in the present work. To be consistent, one can apply a similar expansion to Eq. (4.1) in the effective quadratic potential used in approximating the centroid density,[12,17,18,20] giving

Downloaded 27 Mar 2001 to 18.60.2.110. Redistribution subject to AIP copyright, see http://ojps.aip.org/jcpo/jcpcr.jsp

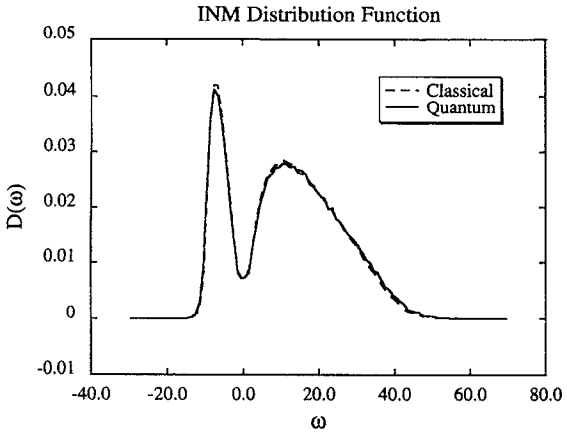

FIG. 1. A plot of the quantum INM spectrum of Eq. (3.9) (solid line) and the classical INM spectrum of Eq. (3.6) (dashed line) for an argon LJ liquid with σ=3.4 Å, ϵ=120 K, m=40 atu, T=156 K, and $\rho\sigma^3$=0.75.

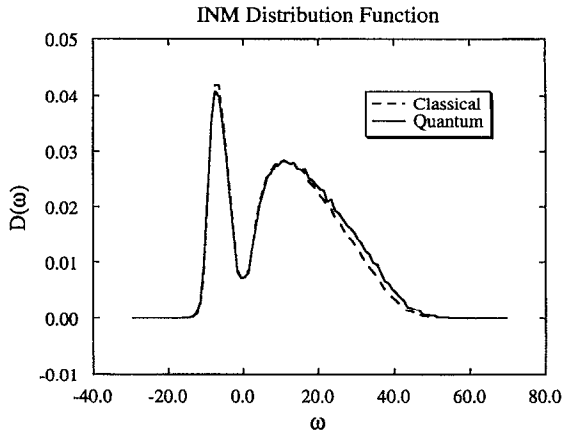

FIG. 2. A plot of the quantum INM spectrum of Eq. (3.9) (solid line) and the classical INM spectrum of Eq. (3.6) (dashed line) for an argon LJ liquid with σ=3.4 Å, ϵ=120 K, m=40 atu, T=144 K, and $\rho\sigma^3$=0.84.

$$\frac{\rho_c(\vec{q}_c)}{\rho_{cl}(\vec{q}_c)}=\prod_l \frac{(\hbar\beta\omega_{c,l}/2)}{\sinh(\hbar\beta\omega_{c,l}/2)}, \tag{4.2}$$

where $\{\omega_l\}$ is the set of frequencies defined by Eq. (2.26) and $\rho_{cl}(\vec{q}_c)$ is the classical density for the particular configuration of centroids $\vec{q}_c$.

In order to carry out the quantum INM analysis, a LJ fluid consisting of 108 particles was studied by a Monte Carlo simulation. After every 1000 Monte Carlo moves, the resulting liquid configuration was used for the normal mode analysis wherein Eq. (4.1) was solved along with Eqs. (2.24)–(2.27) to yield the set of centroid eigenfrequencies $\{\omega_l\}$. The classical frequencies were simply given by the local curvature of the potential. A weighting factor defined by Eq. (4.2) was assigned to each liquid configuration to account for the difference between the classical density and the centroid density. The classical and quantum INM distribution functions were then accumulated over 300 independent liquid configurations.

As argued by Seeley and Keyes,[6] an inspection of the averaged distribution function of normal modes provides a qualitative understanding of certain aspects of liquid-state dynamics. Since it is unclear how to construct a quantitative theory of the self-diffusion constant based on the INM analysis, the goal of this numerical application, and in fact of much of the quantum INM analysis, is to uncover physical insights by comparing the classical and quantum INM distribution functions. In Figs. 1–3, several quantum INM distribution functions of LJ fluids are plotted along with their classical counterparts. Figure 1 corresponds to liquid argon, while Fig. 2 corresponds to a liquid of the argon mass but at a higher density and a lower temperature than the liquid described in Fig. 1. Figure 3 depicts the quantum and classical INM spectra for liquid neon.[32] In all cases, the imaginary frequencies are plotted on the negative frequency axis. As has been suggested, the magnitude of the unstable INMs reveals the known fluidity of the liquid and thus must reflect the self-diffusion process. It is also seen in Figs. 1–3 that the quantum INM distributions manifest a less prominent peak in the imaginary frequency wing than in the classical limit. This strongly suggests a quantum-induced decrease of the self-diffusion constant. Moreover, neon shows a larger change than argon because, as expected, any quantum effects should be inversely proportional to the mass. All these conclusions are in agreement with the results of the centroid MD simulations in Paper II.

B. A solvated quantum particle

The diffusion of a quantum particle such as an electron solvated in a classical fluid is a subject of considerable interest (see, e.g., Refs. 33–38) Path integral simulations have been carried out to study the equilibrium properties of the solvated electron and to investigate its localization behavior (see, e.g., the citations in Refs. 26–28). Such systems are characterized by several factors such as temperature, density, mass of the solvent particles, mass of the solvated particle, solvent–solvent interactions, and solute–solvent interaction.

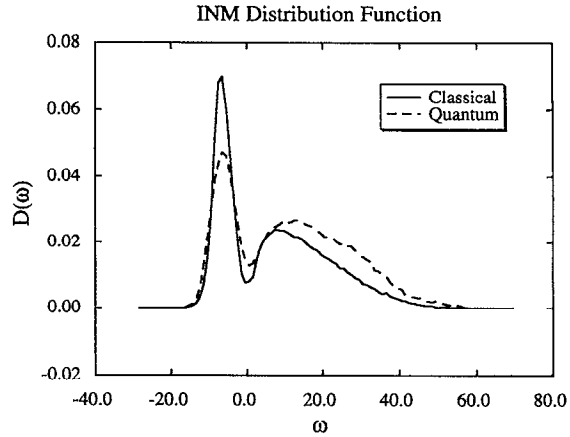

FIG. 3. A plot of the quantum INM spectrum of Eq. (3.9) (solid line) and the classical INM spectrum of Eq. (3.6) (dashed line) for a neon LJ liquid with σ=2.75 Å, ϵ=35.8 K, m=20 atu, T=40 K, and $\rho\sigma^3$=0.68.

Downloaded 27 Mar 2001 to 18.60.2.110. Redistribution subject to AIP copyright, see http://ojps.aip.org/jcpo/jcpcr.jsp

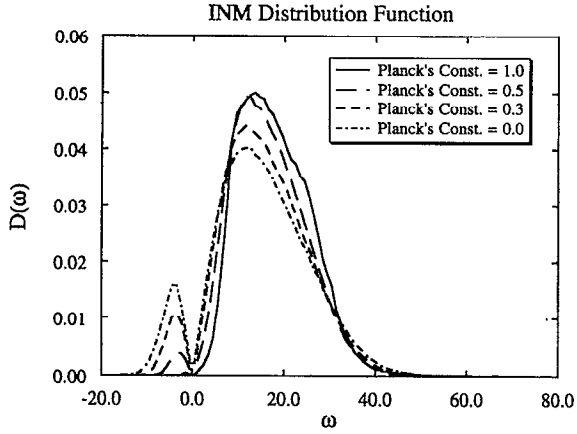

FIG. 4. A plot of the quantum INM spectrum of Eq. (3.9) for the quantum particle in a classical LJ solvent as described in Sec. IV B with $\hbar^*=1.0$ (solid line), $\hbar^*=0.5$ (dashed line), $\hbar^*=0.3$ (dot-dashed line), and $\hbar=0.0$ (dotted line)

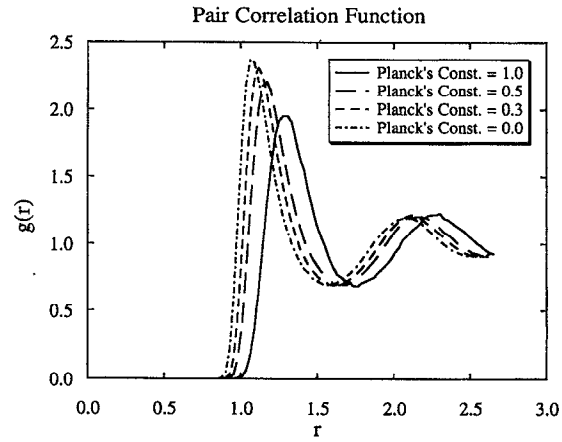

FIG. 5. A plot of the pair correlation between the centroid of the solvated quantum particle and the solvent particles for the same system as shown in Fig. 4.

To simplify the problem in the present case, both of the latter interactions assumed the same LJ potential with $\sigma=1$ and $\epsilon=1.0$. All other variables were parametrized by the LJ width σ, the LJ depth ϵ, and the unit mass $m=1.0$, i.e., $\rho\sigma^3=0.8$, $k_BT/\epsilon=1.0$. The quantum nature of the solute particle was varied by adjusting Planck's constant $\hbar$, namely, $\hbar^* = \hbar/\sqrt{m\sigma^2\epsilon}$ in the reduced units. The solvent consisted of 125 classical LJ particles, and the single solvated quantum particle was located in the center of the periodic box. The system evolved under classical molecular dynamics for a time step of 0.01 with the solvated particle moving on the centroid potential surface. The data were collected over 10^5 time steps after the system was equilibrated. Due to the quantum nature of the solvated particle and the anharmonicity of the interactions, the transcendental equations in Eqs. (2.25)–(2.27) were solved exactly by an iteration method discussed at length in Paper IV.[15]

The quantum INM spectrum of Eq. (3.9) is plotted in Fig. 4 and the pair correlation function between the centroid of the solvated particle and the solvent particles is shown in Fig. 5. The changes in the curves solely reflect the changes in the quantum effects due to the adjustments in the value of $\hbar$. Some comments on these changes are as follows

(a) As $\hbar$ increases in value, the quantum INM spectrum in Fig. 4 is blueshifted, resulting in a larger positive wing and a smaller negative wing. This tendency is usually observed in the classical INM spectrum of a pure fluid when the temperature is decreased, indicating a transition from the liquid phase to solid phase. Since the temperature remains the same in the present case, it is instead a manifestation of the quantum effects, which make it more likely to find the quantum particle in a well region than in a barrier region, leading to less diffusive behavior.

(b) The interpretation in part (a) above is supported by the pair centroid correlation functions $g(r)$ given in Fig. 5, where the outward shift of the main peak with increased $\hbar$ indicates the increase in the effective repulsive radius. In general, the effective centroid potential becomes more repulsive as the solvated particle becomes more quantum mechanical and this change is reflected in the INM spectrum.

(c) As the solvent becomes more dense, a further reduction of the regions of negative curvature in the centroid potential eventually leads to an INM spectrum without any significant density of imaginary frequencies. For the case of $\hbar=1.0$, it is observed that there are essentially no imaginary frequencies. An intuitive interpretation of this limit is that there is no physically accessible transition region for diffusion so that the solvated particle will always be trapped in an effective well with positive frequencies. Naturally, this situation should correspond to a localized solvated quantum particle.[34–39] It is an interesting question whether the critical density and value of $\hbar$ for the imaginary frequencies to vanish corresponds to the situation in which a centroid molecular dynamics calculation[13–15] would also give a vanishing diffusion constant. We hope to address this question in the future.

V. CONCLUDING REMARKS

The present paper builds on our earlier work[12–15] on the path integral centroid perspective in quantum statistical mechanics. The particular focus of the present paper has been to extend the interesting concept of instantaneous normal modes in liquids[5–8] into the quantum regime. Because the quantum dynamics of many-body systems are very difficult to study numerically and/or analytically under any conditions, this extension is a useful one, helping to provide qualitative insight into the behavior of such systems. Specific applications were given to quantum Lennard-Jones fluids and to a quantum solute in a classical Lennard-Jones solvent. The effect of quantum mechanics was to reduce the number of unstable INMs in both cases. In the case of the solvated quantum particle, no unstable normal modes were observed for certain (high) solvent densities, suggesting the INM signature of a localization transition. The analytical aspects of the present theory, as well as its application to more complex systems, remain for future study.

Downloaded 27 Mar 2001 to 18.60.2.110. Redistribution subject to AIP copyright, see http://ojps.aip.org/jcpo/jcpcr.jsp

ACKNOWLEDGMENTS

This research was supported by the National Science Foundation (CHE-9158079). G.A.V. is a recipient of a National Science Foundation Presidential Young Investigator Award, a David and Lucile Packard Fellowship in Science and Engineering, an Alfred P. Sloan Foundation Research Fellowship, and a Dreyfus Foundation New Faculty Award. The authors are indebted to Diane Sagnella for her critical reading of this manuscript.

[1] M. Born and K. Huang, *Dynamical Theory of Crystal Lattices* (Clarendon, Oxford, 1955).
[2] C. Kittel, *Quantum Theory of Solids* (Wiley, New York, 1963).
[3] B. J. Berne and R. Pecora, *Dynamic Light Scattering* (Wiley–Interscience, New York, 1976).
[4] R. Zwanzig, J. Stat. Phys. **9**, 215 (1973).
[5] R. Zwanzig, J. Chem. Phys. **79**, 4507 (1983).
[6] G. Seeley and T. Keyes, J. Chem. Phys. **91**, 5581 (1989).
[7] B. Xu and R. M. Stratt, J. Chem. Phys. **92**, 1923 (1990).
[8] M. Buchner, B. M. Ladanyi, and R. M. Stratt, J. Chem. Phys. **97**, 8522 (1992).
[9] Y. Wan and R. Stratt, J. Chem. Phys. **100**, 5123 (1994).
[10] T. M. Wu and R. F. Loring, J. Chem. Phys. **97**, 8568 (1992).
[11] T. M. Wu and R. F. Loring, J. Chem. Phys. **99**, 8936 (1993).
[12] J. Cao and G. A. Voth, J. Chem. Phys. **100**, 5093 (1994).
[13] J. Cao and G. A. Voth, J. Chem. Phys. **100**, 5106 (1994).
[14] J. Cao and G. A. Voth, J. Chem. Phys. **101**, 6157 (1994).
[15] J. Cao and G. A. Voth, J. Chem. Phys. **101**, 6168 (1994).
[16] R. P. Feynman and A. R. Hibbs, *Quantum Mechanics and Path Integrals* (McGraw–Hill, New York, 1965), pp. 279–286.
[17] R. P. Feynman and H. Kleinert, Phys. Rev. A. **34**, 5080 (1986).
[18] R. Giachetti and V. Tognetti, Phys. Rev. Lett. **55**, 912 (1985); see also, A. Cuccoli, V. Tognetti, P. Verrucchi, and R. Vaia, Phys. Rev. B **45**, 8418 (1992).
[19] G. A. Voth, D. Chandler, and W. H. Miller, J. Chem. Phys **91**, 7749 (1989).
[20] J. Cao and B. J. Berne, J. Chem. Phys. **92**, 7531 (1990).
[21] See Ref. 16, Chap. 10.
[22] R. P. Feynman, *Statistical Mechanics* (Addison–Wesley, Reading, MA, 1972), Chap. 3.
[23] L. S. Schulman, *Techniques and Applications of Path Integration* (Wiley, New York, 1986).
[24] M. S. Swanson, *Path Integrals and Quantum Processes* (Academic, San Diego, 1992).
[25] D. Chandler and P. G. Wolynes, J. Chem. Phys. **80**, 860 (1981).
[26] B. J. Berne and D. Thirumalai, Annu. Rev. Phys. Chem. **37**, 401 (1986).
[27] D. Chandler, in *Liquides, Cristallisation et Transition Vitreuse Les Houches, Session LI*, edited by D. Levesque, J. Hansen, and J. Zinn-Justin (Elsevier, New York, 1991).
[28] J. D. Doll, D. L. Freeman, and T. L. Beck, Adv. Chem. Phys. **78**, 61 (1990).
[29] J. Cao and G. A. Voth, J. Chem. Phys. **99**, 10 070 (1993).
[30] J. P. Hansen and I. M. McDonald, *Theory of Simple Liquids* (Academic, New York, 1986).
[31] In Ref. 16, pp. 303–307; in Ref. 22, pp. 86–96.
[32] D. Thirumalai, R. W. Hall, and B. J. Berne, J. Chem. Phys. **81**, 2523 (1984).
[33] D. Chandler, Y. Singh, and D. M. Richardson, J. Chem. Phys. **81**, 1975 (1984).
[34] A. L. Nichols III, and D. Chandler, J. Chem. Phys. **84**, 398 (1986).
[35] D. Laria and D. Chandler, J. Chem. Phys. **87**, 4088 (1987).
[36] D. Hsu and D. Chandler, J. Chem. Phys. **93**, 5075 (1990).
[37] D. F. Coker, B. J. Berne, and D. Thirumalai, J. Chem. Phys. **86**, 5689 (1987).
[38] B. Space, D. F. Coker, Z. H. Liu, B. J. Berne, and G. J. Martyna, J. Chem. Phys. **97**, 2002 (1992).
[39] J. M. Ziman, *Models of Disorder* (Cambridge University Press, Cambridge, 1979).

Downloaded 27 Mar 2001 to 18.60.2.110. Redistribution subject to AIP copyright, see http://ojps.aip.org/jcpo/jcpcr.jsp